Materials and Design 75 (2015) 40–46

Contents lists available at ScienceDirect

Materials and Design

journal homepage: www.elsevier.com/locate/matdes

Development of Al–Nb–B master alloys using Nb and KBF_4 Powders

M. Nowak [a], W.K. Yeoh [b], L. Bolzoni [a,*], N. Hari Babu [a]

[a] Brunel University London, Institute of Materials and Manufacturing, Brunel Centre for Advanced Solidification Technology, Uxbridge, Middlesex UB8 3PH, UK
[b] Australian Centre for Microscopy & Microanalysis, University of Sydney, Sydney, NSW 2006, Australia

ARTICLE INFO

Article history:
Received 18 September 2014
Revised 5 March 2015
Accepted 7 March 2015
Available online 11 March 2015

Keywords:
Aluminium alloys
Grain refinement
Heterogeneous nucleation
Solidification microstructure
Nb–B inoculation

ABSTRACT

We recently reported that the combined employment of niobium and boron (i.e. Nb-based intermetallics formed in the melt by the addition of powders), instead of niobium or boron individually, is a highly effective way to refine the grain size of Al–Si alloys without the inconvenience of the poisoning effect typical of commercial Al–Ti–B master alloys. In this work the progress concerning the development of Al–xNb–yB master alloys, which are much more suitable for its use in aluminium foundries, is reported and discussed. Precisely, a first approach to produce Al–xNb–yB master alloys as well as its characterisation by means of EDS mapping and TEM is presented. The study is completed by testing the effectiveness of the produced Al–xNb–yB master alloys on pure aluminium and binary Al–10Si alloy as well as commercial hypoeutectic and near-eutectic Al–Si alloys. It is found that the approach employed to produce the Al–xNb–yB master alloys is suitable because the size of the primary α-Al dendrites is significantly reduced in each of the case investigated.
© 2015 The Authors. Published by Elsevier Ltd. This is an open access article under the CC BY license (http://creativecommons.org/licenses/by/4.0/).

1. Introduction

Aluminium (Al) cast alloys are common materials used to fabricate engineering components for the transportation industries, especially the automotive, due to the easiness of their shaping by means of casting processes and the intrinsic reduction of weight of structural components that their employment involve. Moreover, the stringent requirement for the reduction of fuel consumption and, therefore, exhausted gas pollution as well as the design of structural components with lower weight and enhanced mechanical performances are pushing the automotive industry towards the employment of a greater amount of light metals, and Al will definitively play a major role. It is well known that a way to improve static and dynamic mechanical properties of metals is by achieving fine grain structures [1–3]. In the Al industry the practise of grain refinement is well established [1–3] and it generally carried out by the addition of master alloys available in the market which were developed on the ternary Al–Ti–B system [4–15], where different theories to explain the mechanism governing their refinement have been proposed [2,3,10]. In this way, an equiaxed as-cast structure in Al direct chill (DC) casting ingots is achieved which makes the material more suitable for its subsequent downstream processing. This leads to semi-finished products with improved mechanical properties and less cold and hot cracking phenomenon. In the case of Al cast alloys, where silicon (Si) content is generally higher than 4–5 wt.%, the refinement by means of master alloys based on the Al–Ti–X phase diagram (where X = B and C [16–19]) is drastically inhibited due to the formation of titanium silicides. These intermetallics form from the reaction of titanium (Ti) present in the grain refiner and the Si of the alloy. This phenomenon, which is identified as poisoning effect, has been studied in details by many researchers [5,7,20]. Despite this fact, the grain refinement of Al–Si cast alloys is commonly carried out, if done, using commercial Al–Ti–B master alloys due to the lack of effective alternative. We recently reported that efficient and reliable grain refinement of hypo-eutectic and near-eutectic Al–Si cast alloys can successfully be done by employing Nb and B [21–23]. Precisely, the addition of 0.1 wt.% of Nb powder and 0.1 wt.% of B through KBF_4 flux leads to the formation of niobium borides (NbB_2) and niobium aluminides (Al_3Nb) which are responsible for the grain refinement of Al–Si cast alloys (i.e. Nb-B inoculation). Specifically, NbB_2 has a lower lattice mismatch with the Face-Centred Cubic (F.C.C.) structure of Al with respect to TiB_2 whilst Al_3Nb has the same lattice mismatch of Al_3Ti with Al. The greatest difference is, nonetheless, the higher chemical stability of the niobium silicides with respect to titanium silicides. The former intermetallics form at higher temperatures than those generally employed to cast Al–Si alloys. Consequently, Nb–B inoculation should not present any poisoning effect. It is worth mentioning that the addition of a grain refinement in the form of powders at industrial level is not of practical implementation and it is why

* Corresponding author.
E-mail address: leandro.bolzoni@brunel.ac.uk (L. Bolzoni).

http://dx.doi.org/10.1016/j.matdes.2015.03.010
0261-3069/© 2015 The Authors. Published by Elsevier Ltd.
This is an open access article under the CC BY license (http://creativecommons.org/licenses/by/4.0/).

Table 1
Chemical composition of the commercial Al–Si alloys used in the study.

Alloy	Element (wt.%)							
	Al	Si	Fe	Cu	Mn	Mg	Zn	Ti
Pure Al	Balance	0.02	0.08	<0.001	0.001	<0.001	0.002	0.006
Al–10Si	Balance	10.02	0.08	–	0.01	–	0.02	–
LM25 (A356)	Balance	6.5–7.5	0.2	0.2	0.1	0.2–0.4	0.1	0.2
LM6 (A413)	Balance	10.0–13.0	0.6	0.1	0.5	0.1	0.1	0.2

they are generally provided in the form of master alloys. Therefore, the aim of this work is to report and discuss the development of Al–xNb–yB master alloys focusing on the characterisation of the phenomena that take place during their production. The produced Al–xNb–yB master alloys are used to introduce Nb–B inoculants in different Al-based materials (i.e. pure Al, binary Al–Si alloy as well as Al–Si commercial alloys) in order to assess their grain refining potency.

2. Experimental procedure

The materials used to carry out the study about the development of Al–xNb–yB master alloys were pure Al, Nb powder (<45 μm) and potassium tetrafluoroborate (KBF_4). The employment of salt flux like the KBF_4 is a common industrial practise for the production of master alloys (such as the ones based on the Al–Ti–B ternary system). Salt fluxes promote the in-situ formation of borides (i.e. AlB_2 and TiB_2) and titanium aluminide (Al_3Ti) particles (intermetallics) in the Al matrix which constitute the master alloy. Once the master alloy is added to the casting Al alloy, these intermetallic particles (inoculants) act as heterogeneous sites for the nucleation of primary α-Al grains. In the case of the development of the Al–xNb–yB master alloys, the employment of the KBF_4 flux has the advantage that when it reacts with Al generates a significant amount of energy (due to the fact that the reaction is highly exothermic) for a short period of time which locally increases the temperature and helps to dissolve the Nb powder particles. Specifically, the chemical reaction taking place during the mixing of pure Al, pure Nb and KBF_4 are:

$$2KBF_4 + 3Al \rightarrow AlB_2 + 2KAlF_4 \quad (1)$$

$$Nb + 3Al \rightarrow Al_3Nb \quad (2)$$

$$Al_3Nb + AlB_2 \rightarrow NbB_2 + 4Al \quad (3)$$

$$2Nb + 2KBF_4 + 5Al \rightarrow NbB_2 + Al_3Nb + 2KF + 2AlF_3 \quad (4)$$

Three Al–xNb–yB master alloys were produced following the same fabrication route: Al–4Nb–1B, Al–2Nb–1B and Al–1Nb–1B. It is worth mentioning that the real content of Nb and B of the Al–xNb–yB master alloys is thought to be lower because some Nb powder gets oxidised during its addition at high temperature and B recovery from KBF_4 flux at lab scale in not very efficient. That is why the compositions are labelled as "targeted" addition of Nb throughout the whole manuscript. The correct amount of pure Al was placed inside a clay-bonded graphite crucible and melted at 850 °C and left to homogenise during 2 h inside an electric furnace. Subsequently, the Nb powder and the KBF_4 flux were added meanwhile manually stirring the melt with an alumina rod. Stirring was repeated every 15 min during the following 2 h. Finally, the slag present on the surface of the molten metal was removed and the master alloy poured into a pre-heated steel mould. The complete dissolution and reaction of the Nb particles with Al was checked by means of superconductivity experiments. In particular, the magnetic moment was measured as a function of the temperature under a magnetic field of 100 Oe applied by means of a SQUID magnetometer. The cast master alloys were characterised and, therefore, optical micrographs (Axioscope A1 optical microscope), SEM-EDS semi-quantitative chemical analyses (Zeiss Supra 35VP FEG) and TEM (JEOL 2200F) study of the nucleant intermetallic particles were considered. The refining potency and effectiveness of Nb–B inoculation via Al–xNb–yB master alloy addition was tested on different materials like commercially pure Al, binary Al–10Si alloy and commercial Al–Si alloys (i.e. LM25 (A356) and LM6 (A413) alloys). As it can be seen from the chemical composition of the commercial Al–Si alloys shown in Table 1, LM25 is a hypo-eutectic alloy whilst LM6 is a near-eutectic alloy.

Different steel moulds were employed to cast the materials without and with the addition of the Al–xNb–yB master alloys. Specifically, a cone-shaped steel mould (cooling rate ~0.5 °C/s), a 30 mm cylindrical steel mould (cooling rate ~2 °C/s) and the TP-1 mould of the Aluminium Association (cooling rate ~3.5 °C/s) were employed. The classical metallographic route of SiC papers grinding plus OPS polishing was used to prepare the samples for their microstructural analysis. In the case of the determination of the grain size, the polished samples were also anodised passing a current of approximately 10 V/1 A and using a tetrafluoroboric acid (HBF_4) solution. Image analysis to measure the grain size of the cast specimens was carried by means of an Axioscope A1 optical microscope equipped with a dedicated program.

3. Results

3.1. Characterisation of the Al–xNb–yB master alloys

Fig. 1 shows the results of the magnetic moment tests carried out to confirm the complete reaction of Nb with the Al matrix by detection of the superconductivity transformation.

It is well-known that Nb is characterised by a transition (T_c) in its superconductive behaviour at 9.2 K. From the results of the magnetic moment measurements shown in Fig. 1a superconducting transition temperature was detected at 9.2 K when testing the elemental Nb powder. After the combined addition of Nb and potassium tetrafluoroborate powders to Al, the Al–xNb–yB master alloys have not shown the typical transition behaviour to the superconductive state of Nb. This indicates and confirms that Nb completely transforms into Nb-based compounds and it is not present as pure elements in the master alloys anymore.

Fig. 2 shows a representative micrograph of the Al–xNb–yB master alloys produced by mixing pure Al with Nb powder and KBF_4 flux along with the EDS elemental mapping results showing the distribution of the elements that constitute the master alloy.

As it can be seen from the analysis of the micrograph of the Al–xNb–yB master alloys (Fig. 2a), the materials is mainly constituted by the Al matrix and some uniformly dispersed particles are present. The elemental mapping reveals that, as expected, Al is the main constituent (Fig. 2b), Nb is concentrated in many different particles whose distribution is rather uniform (Fig. 2c) and B is

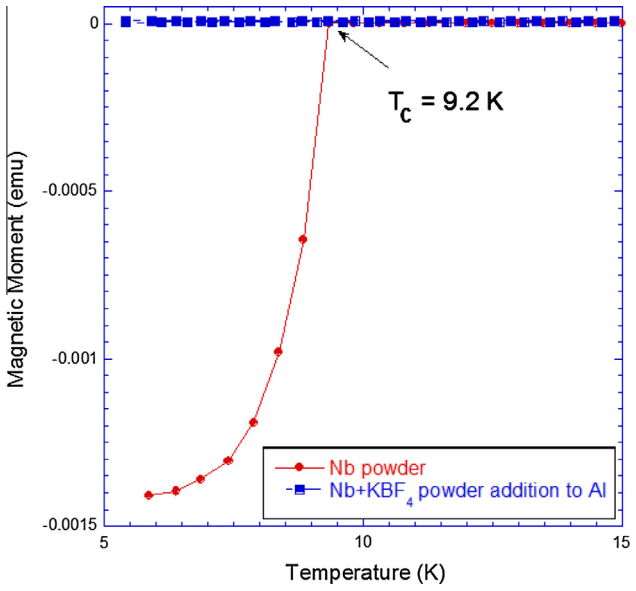

Fig. 1. Magnetic moment as a function of the temperature for Nb powder and Nb + KBF_4 added to Al (i.e. Al–xNb–yB master alloys) (T_c = transition temperature).

uniformly distributed throughout the whole cross-section of the master alloy (Fig. 2d). Specifically, it seems that Nb is primarily present in Nb-based compounds (i.e. niobium borides (NbB_2) and niobium aluminides (Al_3Nb)) whilst B is both present in intermetallic particles as well as dissolved into the Al matrix. Nevertheless, it has to be taken into account that the analysis and quantification of light elements (i.e. from beryllium to fluorine) is limited by inherent physical effects such as the low fluorescence yield, adsorption and peak overlap with L, M and N lines of heavier elements where, specifically, the M line of Nb coincide with the K line of B. It is worth mentioning that the relatively large black spot visible in the Al map (such as in the bottom right corner or in the middle of the sample) are Si particles which were embedded into the soft Al matrix of the Al–xNb–yB master alloys during grinding with SiC papers as checked by EDS analysis.

In order to clarify the nature of the intermetallic particles present in the Al–xNb–yB master alloys, linescan analyses of these potential heterogeneous nucleation sites were performed and an example of the results found is reported in Fig. 3.

From the results of the linescan of the intermetallic particles present in the Al–xNb–yB master alloys there is not a clear understanding of the nature of the particle although it can be said that they are composed of the three elements. Actually, in the centre of the particles the linescan seems to indicate that NbB_2 is present whereas in the outer part of the particles the ratio of the elements is more likely to AlB_2 and Al_3Nb. Moreover, in agreement with the mapping results shown in Fig. 2, Al and B are homogeneously and uniformly distributed throughout the microstructure in both the Al matrix and the intermetallic particle whilst Nb is mainly present in Nb-based compounds (Fig. 3b). TEM analysis of the Al–xNb–yB master alloys was performed and the results of this characterisation are presented in Fig. 4.

From the micrograph of Fig. 4, it can be seen that the intermetallic particles formed due to the interaction between the Nb powder and the KBF_4 flux have a cubic and faceted structure and the great majority of the particles found have a size of around 5 μm. The study of the interface between Nb-based compounds and the Al matrix (Fig. 4b) indicates that this is coherent and it is composed by a layer of Al_3Nb. In particular, it is believed that this layer of Al_3Nb forms on top of the NbB_2 and AlB_2 intermetallic particles that formed during the production of the master alloys. This mechanism was demonstrated for the Al–Ti–B master alloy (i.e. a layer of Al_3Ti forms on the surface of the boride particles (TiB_2) present in the master alloy) using HRTEM [24,25]. Further verification of the nature of the Nb-based intermetallics present in the Al–xNb–yB master alloys and the characterisation of the interphase formed with the α-Al could be obtained using crystallographic orientation relationships via EBSD s and/or Kikuchi line diffraction patterns.

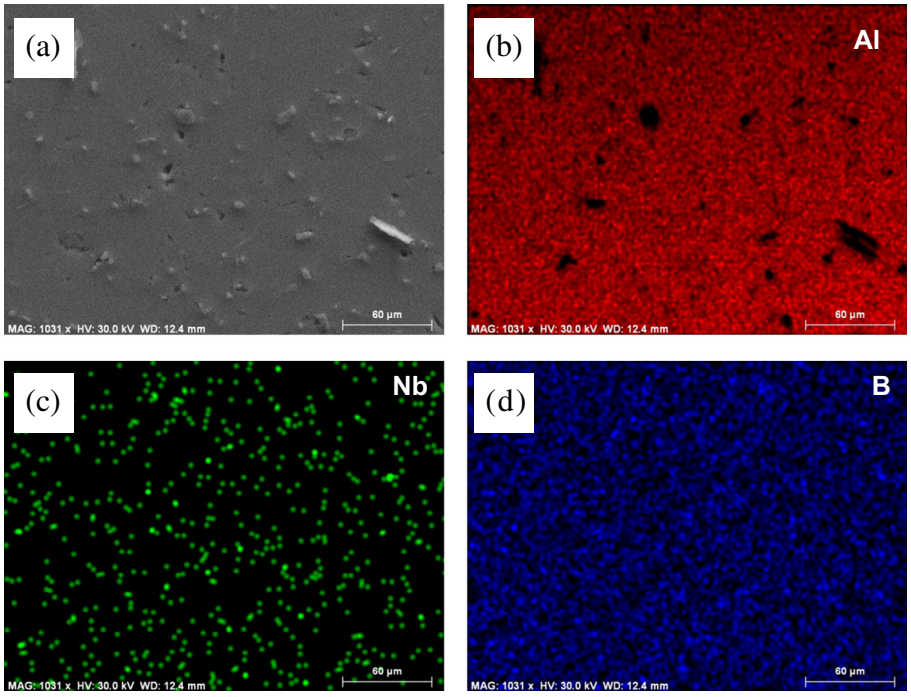

Fig. 2. Representative micrograph and relative EDS mapping of the polished cross-section of the Al–xNb–yB master alloys: (a) BE image, (b) Al map, (c) Nb map and (d) B map.

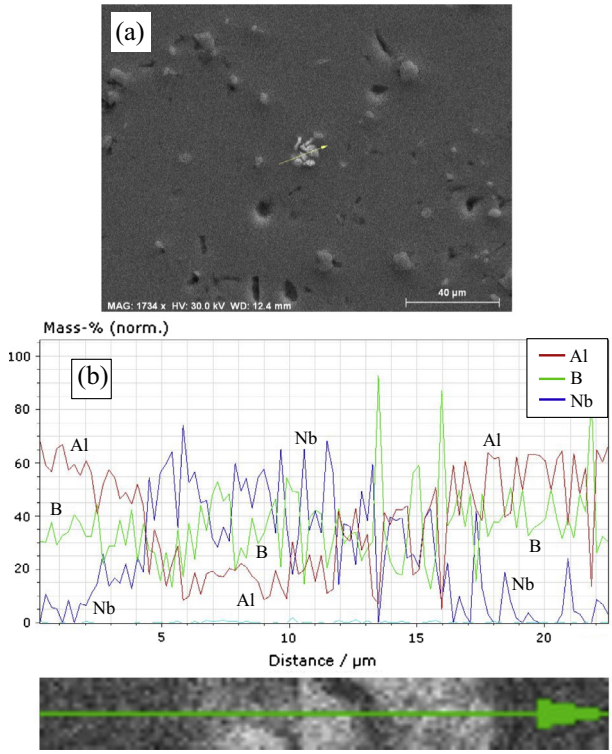

Fig. 3. Representative results of linescan SEM analysis of the intermetallic particles present in the Al–xNb–yB master alloys: (a) BE image and (b) variation of the chemical composition.

3.2. Grain refining potency of Al–4Nb–1B master alloy

In a first set of experiments, the Al–4Nb–1B master alloy was added to the commercial pure Al in order to study its effect. It is worth mentioning that the 4Nb/1B ratio is equivalent to a ideal total amount of 5 wt.% of NbB_2. Nonetheless, this is just a guide because Nb does not only form borides but also aluminides. The amount of master alloy added was equivalent in having a total targeted amount of Nb of 0.1 wt.% as this content demonstrated to have a very powerful grain refinement effect on both pure Al [21] and Al–Si alloys [22]. Fig. 5 shows the anodised micrograph of pure Al without and with the addition of the Al–4Nb–1B master alloy. Specifically, the micrograph was taken in TP-1 test samples (cooling rate ~3.5 °C/s) cast from a pouring temperature of 700 °C.

As it can be seen in Fig. 5a, the TP-1 samples of commercially pure Al without the addition of any grain refiner is characterised by coarse equiaxed grain of approximately 2300 µm in size. The addition of 0.1 wt.% equivalent Nb (Fig. 5b) via Al–4Nb–1B master alloy addition significantly reduces the final grain size in the order of hundreds of microns and does not change the morphology of the Al grain, which remains equiaxed. The results shown in Fig. 5 are in agreement with the results found when adding Nb powder + KBF_4 flux directly to the melt [21–23] instead of an Al–4Nb–1B master alloy confirming the grain refiner potency of Nb–B inoculation. From Fig. 5, it can also be seen that the reduction in grain size obtained through the addition of the Al–4Nb–1B master alloy is comparable to that of the commercial Al–5Ti–1B master alloy (Fig. 5c). Nonetheless, it is important to remark the to obtain such refinement a much higher addition rate had to be used due to the fact that Nb has a much lower growth restriction factor in Al with respect to that of Ti [26].

Fig. 6 shows the results of the characterisation of the commercial hypoeutectic LM25 (A356) alloy prior and after the addition of Nb–B inoculants by means of the Al–4Nb–1B master alloy as well as Nb and KBF_4 powders. In particular, the results refer to the materials cast at 680 °C using a TP-1 mould (cooling rate ~3.5 °C/s).

From the analysis of the anodised micrograph shown in Fig. 6, it can be seen that the microstructure of the LM25 alloy without the addition of grain refiners (Fig. 6a) is composed of primary α-Al dendrites of approximately 1000 µm. After the addition of the Nb–B inoculants (Fig. 6b and c), the size of the Al dendrites is significantly reduced (~300 µm). Although comparable, it can be noticed that the grain size of the LM25 alloy refined by the addition of powders (Fig. 6c) is slightly finer in comparison to the addition of the Al–4Nb–1B master alloy (Fig. 6b). This difference seems to be dictated by the relative amount and nature of the potential heterogeneous nucleation substrates present because of the influence of the different Nb/B ratio.

Experiments without and with the addition of the Al–4Nb–1B master alloy were performed on the near-eutectic LM6 (A413) alloy from the pouring temperature of 680 °C. In this case a preheated (200 °C) permanent steel mould was used (cooling rate ~2 °C/s) and the total equivalent amount of ideal NbB_2 particles added to the melt was varied in the 0.025–0.2 wt.% range. The results of the measurements of the grain size performed on the cross-section of the LM6 samples are summarised in Fig. 7.

From the measurements of the primary α-Al dendrites size shown in Fig. 7, it can be noticed that the grain size decreases with the increment of the equivalent amount of Nb added to the molten

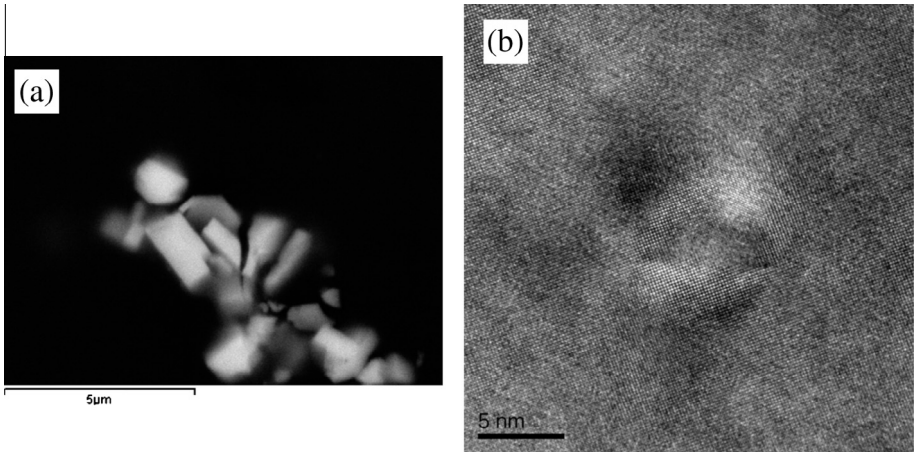

Fig. 4. Results of the characterisation carried put on the intermetallic particles present in the Al–xNb–yB master alloys: (a) SEM image and (b) bright field TEM image.

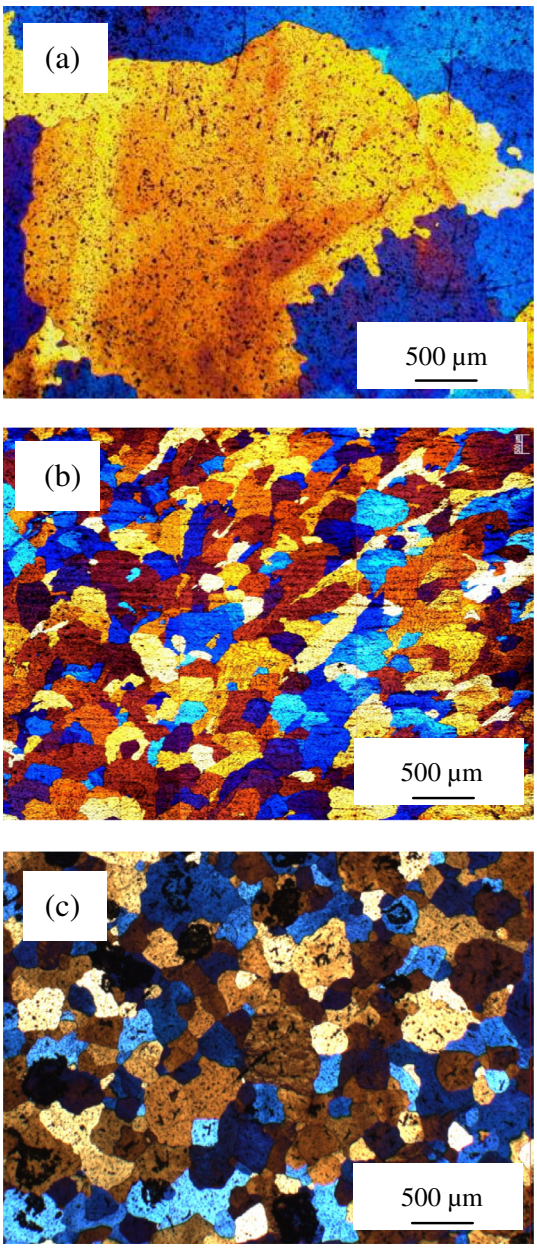

Fig. 5. Anodised micrograph showing the mean grain size of commercially pure Al TP-1 test samples cast from 700 °C: (a) reference, (b) 0.1% targeted Nb (Al–4Nb–1B master alloy) and (c) 0.1% of Al–5Ti–1B master alloy.

metal. This is because the greater the amount of ideal NbB_2 added, the higher the content of intermetallics particles (i.e. Nb-based compounds) available to act as inoculants for the heterogeneous nucleation of the primary dendrites. Specifically, the grain size decreases following an asymptotic trend with the increment of the ideal NbB_2 addition and stabilises for targeted addition higher than 0.1 wt.%. Comparable grain size in the LM6 alloy was obtained when adding an Al–2Nb–2B master alloy [27].

3.3. Grain refining potency of Al–2Nb–1B master alloy

The refining potency of the Al–2Nb–1B master alloy was assessed by considering two targeted levels of addition (i.e. 0.025 wt.% and 0.1 wt.% of Nb) to the binary Al–10Si alloy cast at 740 °C using a cone-shaped permanent mould (cooling rate ~0.5 °C/s) and the results are presented in Fig. 8.

From Fig. 8, the addition of the Al–2Nb–1B master alloy has similar grain refining effect as the other Al–xNb–yB master alloys and, thus, the grain size decreases along with the increment of the targeted Nb content.

3.4. Grain refining potency of Al–1Nb–1B master alloy

The efficiency of the Al–1Nb–1B master alloy was checked on the LM6 alloy was cast at 740 °C into a steel cone-shaped mould (cooling rate ~0.5 °C/s) ranging the level of addition from 0.01 wt.% to 0.1 wt.% of targeted Nb. The variation of the grain size with the amount of Al–1Nb–1B master alloy addition is shown in Fig. 9.

From the analysis of the variation of the grain size of the LM6 samples cast form 740 °C (Fig. 9), it can be seen as in the previous case the grain size of the primary Al dendrites decreases with the increment of the total amount of Nb and B added or, conversely, to the total amount of inoculant particles available as potential heterogeneous nucleation sites. More in detail, the reference materials is characterised by quite a coarse grain size (~2000 μm) which diminishes down to around 300 μm with the addition of 0.1 wt.% of targeted Nb.

4. Discussion

The production of Al–xNb–yB master alloys by means of Nb powder and KBF_4 flux added to molten Al at 850 °C seems to be a suitable and efficient way. In particular, EDS mapping of the element that constitutes the master alloys reveals that Nb is mainly concentrated in the intermetallic particles (i.e. NbB_2 and Al_3Nb) which forms upon the dissolution of Nb powder particles into the melt. Conversely, B is uniformly distributed throughout the whole material and it is, therefore, thought to be present in both borides and in solid solution. Linescan of the intermetallic particles confirmed the formation of both borides (NbB_2 and AlB_2) and aluminides (Al_3Nb) whilst TEM analysis indicates that a coherent interface is present between Al_3Nb and Al. As presented in the discussion of the discovery of the potency of Nb–B inoculation for the refinement of Al–Si alloys [21,22], the Al–Nb–B phase diagram is characterised by significant analogies with the Al–Ti–B phase diagram on the base of which the commercial Al–Ti–B master alloys were developed. Consequently, by combining the knowledge of the nucleation theories proposed [2,3,10] with the data available in the literature and the results presented in Section 3, it is inferred that when the Al–Nb–B master alloy is added to the molten metal, NbB_2 and Al_3Nb particles spread into the molten metal. On the base of the work performed by Bunn et al. [25], possibly nucleation occurs only on the basal plane {0001} of the hexagonal NbB_2 particles which are coated with a three-atomic layer of Al_3Nb. This fact is in agreement with TEM results (Fig. 4) and the results of the linescan shown in Fig. 3 where the inner part of the intermetallic particle analysed had a chemical composition which resembles that of NbB_2 whereas the outer part was richer in Al (i.e. Al_3Nb). Similarly to the case of Al–Ti–B, the nucleation of Al grains is taking place via enhanced heterogeneous nucleation and the mechanism can be described considering specific orientation relationships. Nucleation of the primary α-Al dendrites is thought to happen in the following specific parallel close packed directions and planes:

$$\{1\,1\,1\}_{Al} \| \{1\,1\,2\}_{Al_3Nb} \| \{0\,0\,0\,2\}_{NbB_2} \quad (5)$$

$$\langle\langle 1\,\bar{1}\,0\rangle Al \| \langle 2\,0\,\bar{1}\rangle Al_3Nb \text{ or } \langle 1\,\bar{1}\,0\rangle Al_3Nb \| \langle 1\,1\,\bar{2}\,0\rangle NbB_2 \quad (6)$$

It is worth remembering that the lattice mismatch at the α-Al/Al_3Nb interphase is much smaller than that at the α-Al/NbB_2 interphase [21] and it is, therefore, easier to form a coherent interphase

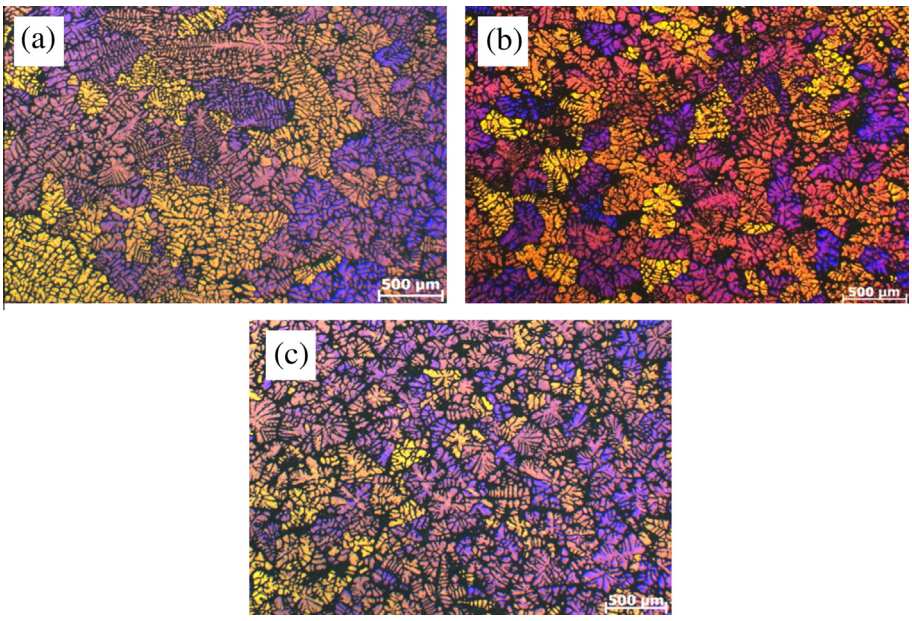

Fig. 6. Anodised micrograph of the LM25 (A356) alloy TP-1 samples cast from 680 °C: (a) reference, (b) 0.1% targeted Nb (Al–4Nb–1B master alloy) and (c) 0.1% targeted Nb (0.1% Nb powder + 0.1% B via KBF_4 flux).

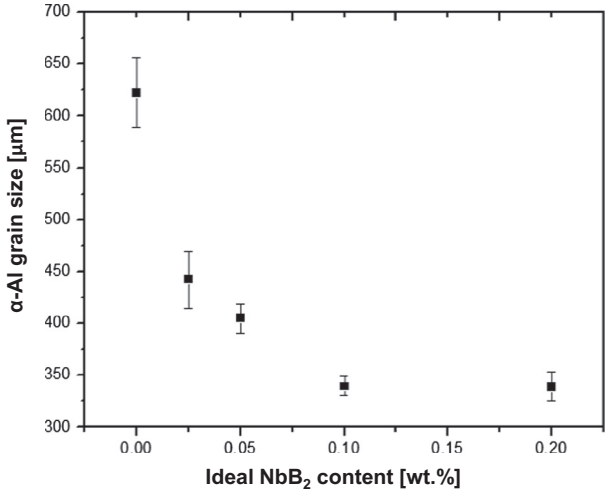

Fig. 7. Variation of the grain size of the LM6 (A413) alloy cast from 680 °C as a function of the ideal NbB_2 content added to the melt by means of the Al–4Nb–1B master alloy.

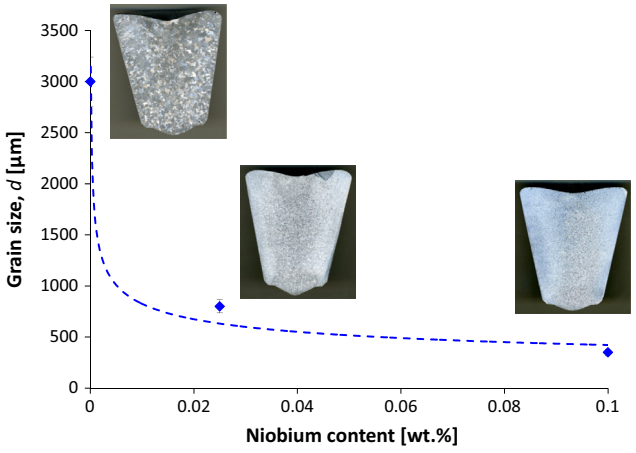

Fig. 8. Variation of the grain size of the binary Al–10Si alloy cast at 740 °C with the amount of targeted Nb added by means of the Al–2Nb–1B master alloy.

in the former case than in the latter. That is why it is thought that NbB_2 constitute the actual potential heterogeneous nucleation substrates on top of which a layer of Al_3Nb is formed as a transition layer to favour the nucleation of α dendrites.

The trial production of Al–xNb–yB master alloys on different materials such as pure Al, binary Al–10Si alloy and commercial Al–Si alloys confirm that the Nb–B inoculation has a significant grain refining potency for the heterogeneous nucleation of Al. More in detail, Al–Nb–B master alloys can refine pure Al (Fig. 5) to similar grain size level obtained thought the employment of commercial Al–Ti–B master alloys. Nonetheless, the addition ratio to reach comparable results is significantly higher which is due to much lower growth restriction factor of Nb with respect to Ti [26]. Independently of the relative ratio of Nb/B of the produced master alloys, Nb–B inoculation permits to efficiently refine the microstructural features of hypoeutectic (i.e. Al–10Si and LM25 alloys) and near-eutectic (i.e. LM6 alloy). Specifically, the grain size decreases with the increment of the targeted Nb content following a power-law trend (Figs. 8 and 9) where grain sizes in the range of 300–400 µm are attained by means of the addition of 0.1 wt.% Nb (targeted). It is worth remembering that the actual content of Nb and B in the Al–xNb–yB master alloys is lower than the expected on the base of the initial composition. Moreover, by these trails of the production of Al–xNb–yB master alloys it is demonstrated that the master alloys have the same grain refining potency of the direct addition of Nb powder and KBF_4 flux to the molten alloy to be refined and they could then be applied at industrial level. From the comparison of the performances of the different Al–xNb–yB master alloys added to various Al–Si alloys cast with diverse addition rates and cast from relatively low (680°) and more industrially similar (740°) temperatures it is found that the Nb/B ration influences the performances of Nb–B inoculation due to the total amount of Nb-based compounds that can form. The efficient and reliable refinement of as-cast structure would lead to the fabrication of engineered components with improved performances. Conversely, lightweight structural products with more isotropic behaviour (i.e. less dependent on the nature of the solidification) could be design using the refined as-cast Al–Si alloys.

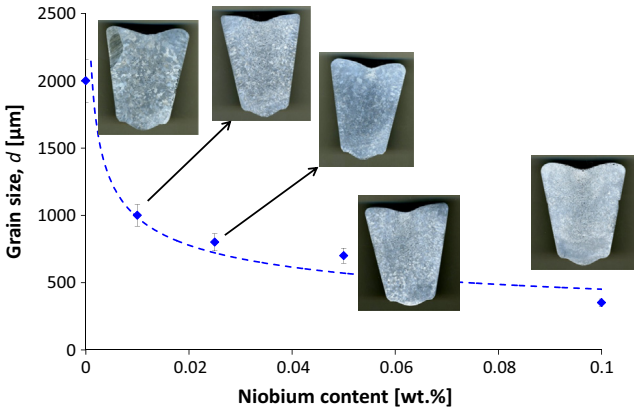

Fig. 9. Variation of the grain size of the LM6 alloy cast at 740 °C with the amount of targeted Nb added by means of the Al–1Nb–1B master alloy.

5. Conclusions

From this study about the trial production of Al–xNb–yB master alloys starting from niobium powder and KBF_4 flux it can be concluded that the process and parameters employed are sufficiently good to fabricate the proposed master alloys because niobium is completely dissolved and present only in niobium-based compounds. Nonetheless, optimisation of the Nb powder addition to prevent its oxidation, better B recovery from the KBF_4 flux and appropriate mixing procedure are some of the point that could be improved to enhance the quality and reliability of the Al–xNb–yB master alloys. This work also demonstrates that the addition of these Al–xNb–yB master alloys to aluminium and its alloy introduces potent Nb–B inoculants which promote the refinement of the grain structure via heterogeneous nucleation. Nb–B inoculation is effective in different Al–Si cast alloys solidified under various conditions (i.e. pouring temperatures and cooling rates) although there is an influence by the targeted Nb/B ratio, relation that has to be optimised.

Acknowledgements

The authors are thankful for the financial support from the Engineering and Physical Sciences Research Council (EPSRC) through the EP/J013749/1 and EP/K031422/1 Projects and the Technology Strategy Board (TSB) through the TSB/101177 Project.

References

[1] E.L. Rooy, Aluminum and Aluminum Alloys, Castings, 15, ASM International, Ohio, 1988.
[2] D.G. McCartney, Grain refining of aluminium and its alloys using inoculants, Int. Mater. Rev. 34 (1989) 247–260.
[3] B.S. Murty, S.A. Kori, M. Chakraborty, Grain refinement of aluminium and its alloys by heterogeneous nucleation and alloying, Int. Mater. Rev. 47 (2002) 3–29.
[4] G.K. Sigworth, The grain refining of aluminum and phase relationships in the Al–Ti–B system, Metall. Trans. A 15 (1984) 277–282.
[5] G.K. Sigworth, M.M. Guzowski, Grain refining of hypoeutectic Al–Si alloys, AFS Trans. 93 (1985) 907–912.
[6] M.M. Guzowski, G.K. Sigworth, D.A. Sentner, The role of boron in the grain refinement of aluminum with titanium, Metall. Trans. A 18 (1987) 603–619.
[7] T. Sritharan, H. Li, Influence of titanium to boron ratio on the ability to grain refine aluminium–silicon alloys, J. Mater. Process. Technol. 63 (1997) 585–589.
[8] A.L. Greer, P.S. Cooper, M.W. Meredith, W. Schneider, P. Schumacher, J.A. Spittle, et al., Grain refinement of aluminium alloys by inoculation, Adv. Eng. Mater. 5 (2003) 81–91.
[9] S. Nafisi, R. Ghomashchi, Grain refining of conventional and semi-solid A356 Al–Si alloy, J. Mater. Process. Technol. 174 (2006) 371–383.
[10] M. Easton, D.H. St. John, Grain refinement of aluminum alloys: Part I. The nucleant and solute paradigms – a review of the literature, Metall. Mater. Trans. A 30 (1999) 1613–1623.
[11] G.P. Jones, J. Pearson, Factors affecting grain refinement of aluminium using Ti and B additives, Metall. Mater. Trans. B 7 (1976) 223–234.
[12] D.H. St. John, L.M. Hogan, Al3Ti and the grain refinement of aluminum, J. Aust. Inst. Met. 22 (1977) 160–166.
[13] M.S. Lee, B.S. Terry, Effect of processing parameters on a luminide morphology in aluminium grain refining master alloy, Mater. Sci. Technol. 7 (1991) 608–612.
[14] C.D. Mayes, D.G. McCartney, G.J. Tatlock, Influence of microstructure on grain refining performance of Al–Ti–B master alloys, Mater. Sci. Technol. 9 (1993) 97–103.
[15] A. Hardman, F.H. Hayes, Al–Ti–B grain refining alloys from Al, B_2O_3 and TiO_2, Mater. Sci. Forum 247 (1996) 217–222.
[16] B.T. Gezer, F. Toptan, S. Daglilar, I. Kerti, Production of Al–Ti–C grain refiners with the addition of elemental carbon, Mater. Des. 31 (2010) S30–S35.
[17] P. Li, S. Liu, L. Zhang, X. Liu, Grain refinement of A356 alloy by Al–Ti–B–C master alloy and its effect on mechanical properties, Mater. Des. 47 (2013) 522–528.
[18] Y. Zhang, N. Ma, H. Wang, X. Li, Study on damping behavior of A356 alloy after grain refinement, Mater. Des. 29 (2008) 706–708.
[19] E. Samuel, B. Golbahar, A.M. Samuel, H.W. Doty, S. Valtierra, F.H. Samuel, Effect of grain refiner on the tensile and impact properties of Al–Si–Mg cast alloys, Mater. Des. 56 (2014) 468–479.
[20] M.N. Binney, D.H. St. John, A.K. Dahle, J.A. Taylor, E. Burhop, P.S. Cooper, Grain refinement of secondary aluminium–silicon casting alloys, Light Met. (2003).
[21] M. Nowak, L. Bolzoni, N. Hari Babu, Grain refinement of Al–Si alloys by Nb–B inoculation. Part I: concept development and effect on binary alloys, Mater. Des. 66 (2015) 366–375.
[22] L. Bolzoni, M. Nowak, N. Hari Babu, Grain refinement of Al–Si alloys by Nb–B inoculation. Part II: application to commercial alloys, Mater. Des. 66 (2015) 376–383.
[23] L. Bolzoni, M. Nowak, N. Hari Babu, Grain refining potency of Nb–B inoculation on Al–12Si–0.6Fe–0.5Mn alloy, J. Alloys Compd. 623 (2015) 79–82.
[24] B.J. Mc Kay, P. Schumacher Heterogeneous nucleation mechanisms of TiB2 particles in Al alloys, TMS 2005 (2005) 155–164.
[25] A.M. Bunn, P. Schumacher, M.A. Kearns, C.B. Boothroyd, A.L. Greer, Grain refinement by Al–Ti–B alloys in aluminium melts: a study of the mechanisms of poisoning by zirconium, Mater. Sci. Technol. 15 (1999) 1115–1123.
[26] M. Easton, D. St. John, An analysis of the relationship between grain size, solute content, and the potency and number density of nucleant particles, Metall. Trans. A 36 (2005) 1911–1920.
[27] L. Bolzoni, M. Nowak, N. Hari Babu, Assessment of the influence of Al–2Nb–2B master alloy on the grain refinement and properties of LM6 (A413) alloy, Mater. Sci. Eng. A 628 (2015) 230–237.